

# Dynamic characteristics of base-isolated reactor building subjected to various types of travelling waves

I.Takahashi, Y.Koyanagi, N.Fukuwa & K.Yoshida

*Ohsaki Research Institute, Shimizu Construction Co. Ltd, Tokyo, Japan*

## 1 INTRODUCTION

Studies on the base isolation systems applied to nuclear reactor building have been reported recently (Kunar 1979). In the isolation systems, laminated elastomer bearing pads (LEBPs) are widely used to decrease the responses of structure by lengthening the natural period (Jolivet 1977). Therefore, the characteristics of input earthquake motions should be studied in the seismic design of isolated structures. Most of the devices having LEBPs are effectively operated only for the horizontal motion, but they are ineffective for the vertical or rocking motions. For the structure subjected to seismic waves with phase difference, such as obliquely incident waves or surface waves, the rocking and torsional movements of the structure are additionally produced. However, there have been few studies on the responses of the structure with the base isolation systems subjected to the motion with phase difference (Richili 1981, Wolf 1983).

This paper describes the earthquake response analysis of a typical BWR MARK-II type reactor building supported by the laminated elastomer pads, which is subjected to obliquely incident SH and SV waves. Dynamic characteristics of the base-isolated reactor building and base isolation device are investigated. In order to solve this problem, the frequency domain analyses are carried out for a linear system using the substructure technique where the soil system is analyzed by boundary element method (Yoshida 1984) and the structure is modeled by a spring-mass system. Since the sliding characteristics are greatly influenced by variation of axial forces when the structure is subjected to SV wave, nonlinear analyses are further conducted for a reactor building supported by sliding laminated elastomer bearing pads (SLEBPs).

## 2 INVESTIGATION ON THE STRUCTURE SUPPORTED BY LAMINATED ELASTOMER BEARING PADS

### 2.1 Analytical model and conditions

A BWR MARK-II type reactor building on the half-space medium shown in Fig.1 is chosen as a typical model. This reactor building is assumed to have no eccentricity, and is supported by 1,600 LEBPs which are set up at equal distance between the two square bases. The isolation frequencies of LEBPs are assumed to be 1.0Hz and 0.5Hz for the horizontal motion, 20.0Hz for the vertical motion. The damping factors of both the reactor building and isolation device are 5%.

The Input earthquake motion is generated artificially and its maximum acceleration amplitude is 286Gal. The incidence angles of SH and SV waves are selected as 0°, 10°, 20° and 30°. The analyses are carried out using the dynamic substructure technique in the frequency domain.

In Tables 1 and 2, the properties of soil and isolation devices are indicated. Figs.2 and 3 show the time history and response spectrum of the input earthquake motion, respectively.

## 2.2 Results of analysis

The foundation input motions are shown in Figs.4 and 5 in the form of transfer functions. They indicate that the torsional and rocking motion are excited by obliquely incident SH and SV waves, respectively.

The dynamic response of the reactor building subjected to SH and SV waves are shown in Figs.6 and 7, respectively. Those results are compared with those for a non-isolated reactor building. When the isolated structure is subjected to vertical incident SH or SV waves, the response curves have sharp peaks only at the isolation frequency, while the responses are suppressed in the other frequency range. However, when the isolated structure is subjected to obliquely incident SV waves, the response curves have second peaks caused by the rocking motion. As the incidence angle increases, the responses are getting large not only at the isolation frequency but also in the other frequency range.

Next the results of the earthquake response analyses are considered. The maximum response accelerations of the base-isolated and non-isolated reactor buildings subjected to SH waves are shown in Fig.8 in the case of  $f_H = 1.0\text{Hz}$ . The isolated reactor building moves horizontally as like a rigid body, and the horizontal motion decrease considerably. LEBPs are also effective to decrease the torsional motion which contributes to the horizontal motion at most 10%. The maximum response to SV waves is shown in Fig.9. The horizontal responses at the top of the structure are increased and furthermore, the vertical motion of the structure is generated considerably by obliquely incident SV waves.

In Tables 3 and 4, the maximum values of the horizontal or vertical response accelerations at a height of 50.5m are indicated. The response caused by the horizontal, torsional and rocking motion of the base are also shown. When the base-isolated structure is subjected to obliquely incident SH waves, the responses are independent of the incidence angle. When subjected to SV waves, however, the responses are increased by the rocking motion as the incidence angle becomes large. Especially in the case of the incidence angle  $\theta = 30^\circ$ , which is more than the critical angle ( $24^\circ$ ), the horizontal accelerations caused by the rocking motion are over 150 gal whether or not the isolation device is provided. It is indicated that this type of isolation system is not effective to reduce the rocking motion.

Figs.10 and 11 show the floor response spectra. While the responses of the structure subjected to SH waves vary little according to the incidence angle, those to SV waves with a fairly large incidence angle increase by the rocking motion in the high frequency range. These results coincide with the tendency of the transfer functions.

The responses of the isolation devices are discussed as follows. Tables 5 and 6 show the maximum values of the relative horizontal displacement, and the relative torsional angle between the upper and lower bases. Obliquely incident SH waves produce the relative torsional angle, consequently the horizontal displacement increases at the edge of the base. However, even when the structure is subjected to SH wave with the incidence angle of  $30^\circ$ , the relative horizontal displacement increases only about 5%. Thus, it is pointed out that the torsional motion produced by obliquely incident SH waves have little effect on the responses of the isolation devices.

In the case of SV waves, the rocking motion is produced. Therefore, the vertical motion are enlarged at the edge. When the structure is subjected to SV waves with the incidence angle of  $30^\circ$ , the maximum relative vertical displacement is about 0.03cm and then, the axial forces of the isolation devices amount to about 95ton at the edge of the base. From these results, it becomes clear that the axial forces of the isolation devices possibly vary from 0.5 to 1.5 times of those produced by the weight of the structure.

### 3 INVESTIGATION ON THE STRUCTURE SUPPORTED BY SLIDING LAMINATED ELESTOMER BEARING PADS

From the results mentioned above, the axial forces of LEBPs possibly vary with the position when subjected to obliquely incident SV waves. Therefore, if the isolation systems consist of LEBPs, the friction forces of the pads may be different each other. In this section non-linear characteristics of structural responses caused by the variation of axial forces are investigated. The analyses are carried out using the substructure technique in time domain under the same conditions as those for the previous study. In this study, the dynamic impedance functions are simplified to the additional mass, viscous damping coefficient and stiffness evaluated at the isolation frequency. The force-displacement relationship of the isolation devices is shown in Fig.12. The horizontal motion of the isolation device is coupled with the axial force, and the device slides horizontally when the horizontal strains reach to the friction forces. The friction coefficient of the isolation device is assumed to be 0.2.

Fig.13 and Table 7 show the maximum horizontal and vertical response accelerations of the structure. When the structure is subjected to SV wave with a small incidence angle, similar tendency of the dynamic characteristics is recognized whether or not the sliding plates exist. However, there is a little difference when the incident angle is large. The horizontal floor response spectra are shown in Fig.14. It is indicated that the peaks at  $f_H=1.0\text{Hz}$  are reduced considerably by sliding of the isolation devices. Table 8 shows the maximum relative displacement between the upper and lower bases. The relative vertical displacement shows a tendency to increase. On the contrary, the relative rocking angle tends to decrease in comparison with the results of the structure supported by LEBPs. However, as the incidence angle increases, the both relative horizontal displacement and rocking angle become large. Figs.15 and 16 show the maximum axial force distribution of the isolation devices. The axial force distribution depends largely on the position within the base.

### 4 CONCLUSIONS

The dynamic characteristics of the base-isolated reactor building is studied. The results of this study is summerized as follows,

- (1) The isolation devices supported by laminated elastomer pads are effective for decreasing the horizontal and torsional motions. However, they are ineffective for the vertical or rocking motions,
- (2) The vertical axial force of the isolation devices possibly vary from 0.5 to 1.5 times of the axial force produced by weight of the structure,
- (3) The characteristics of the structure supported by sliding laminated elastomer bearing pads are similar to those of the laminated elastomer bearing pads.

### REFERENCES

- Jolivet, F. et al., 1977, "Aseismic Foundation System for Nuclear Power Stations," Proc. of the 4th SMiRT, K9/2, San Francisco, USA
- Kunar, R., R. et al., 1979, "A Review of Seismic Isolation for Nuclear Structures" Special Report of Elastic Power Research Institute
- Yoshida, K., et al., 1984, "Dynamic Response of Rigid Foundations Subjected to Various Types of Seismic Wave" Proc. of the 8th WCEE, Vol. III, pp.745-752, San Francisco, USA
- Richili, M., et al., 1981, "Effect of Travelling Waves on a Shock Isolated Nuclear Power Plant Put on Rock Foundation," Proc. of the 6th SMiRT, K12/7, Paris, France
- Wolf, J., P. et al., 1983, "Response of a Nuclear Power Plant on Aseismic Bearing from Horizontally Propagating Waves" Proc. of the 7th SMiRT, K16/1, Chicago, USA

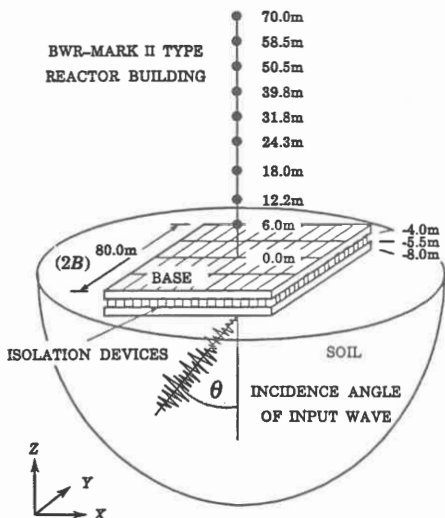


Figure 1. Description of model

Table 1. Properties of soil

	Constant
Shear Wave Velocity	1,000 m/sec
Poisson's Ratio	0.4
Damping Factor	0.02
Weight per Volume	2.0t/m <sup>3</sup>

Acceleration (Gal)

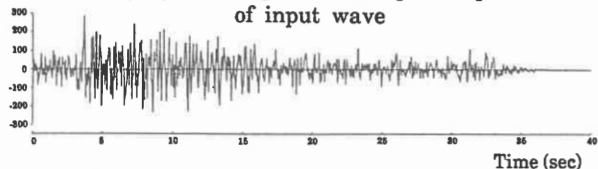
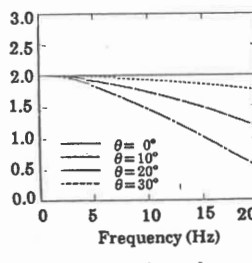
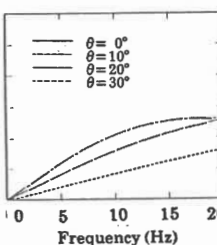


Figure 2. Time history of input wave



(a) Horizontal



(b) Torsional

Figure 4. Foundation input motions due to SH waves

Table 2. Properties of isolation devices

	Case-I	Case-II
Isolation Frequency for Horizontal Motion $f_H$ (Hz)	1.0	0.5
Isolation Frequency for Vertical Motion $f_V$ (Hz)	20.0	20.0
Total Horizontal Spring Constant $K_H$ (t/m)	$1.13 \times 10^6$	$2.82 \times 10^5$
Total Vertical Spring Constant $K_V$ (t/m)	$4.52 \times 10^8$	$4.52 \times 10^8$
Total Rocking Spring Constant $K_R$ (t-m)	$2.41 \times 10^{11}$	$2.41 \times 10^{11}$
Total Torsional Spring Constant $K_T$ (t-m)	$1.20 \times 10^9$	$3.01 \times 10^8$

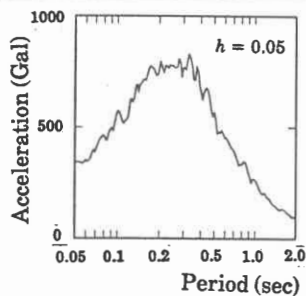
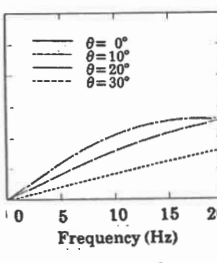
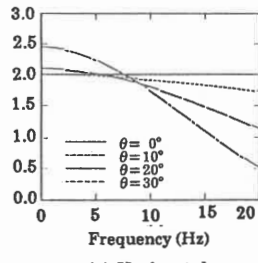


Figure 3. Response spectrum of input wave

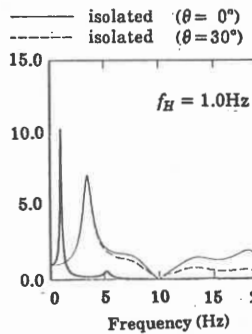


(a) Horizontal

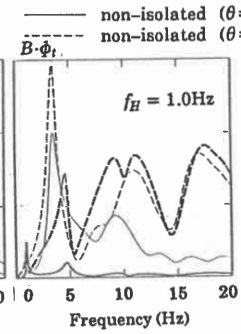


(b) Rocking

Figure 5. Foundation input motions due to SV waves

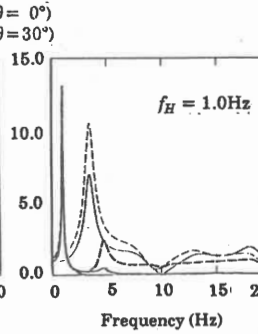


(a) Horizontal (E.L. 50.5m)

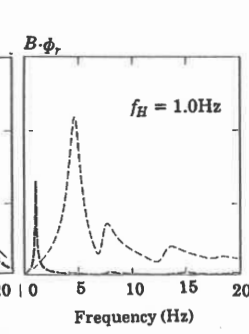


(b) Torsional (Upper Base)

Figure 6. Transfer functions due to SH waves

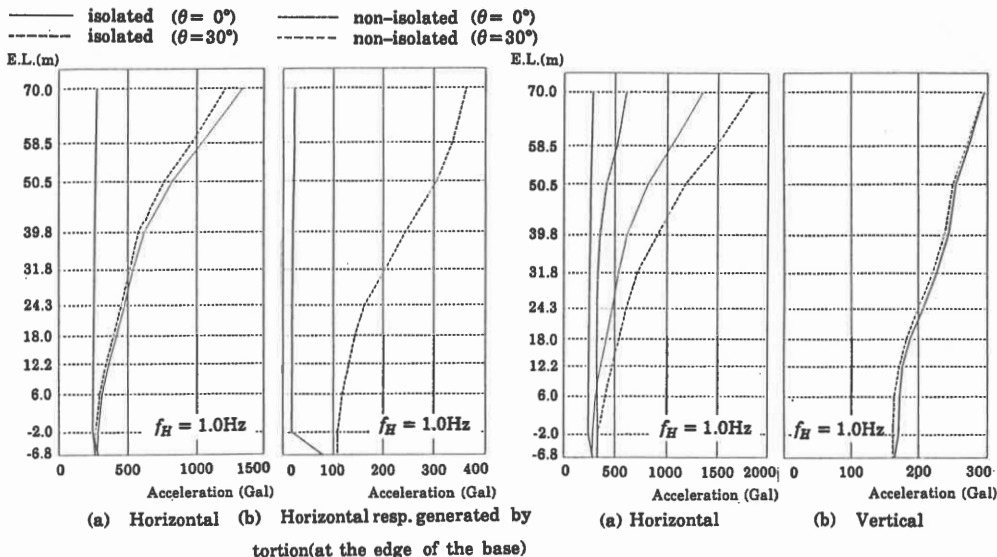


(a) Horizontal (E.L. 50.5m)



(b) Rocking (Upper Base)

Figure 7. Transfer functions due to SV waves



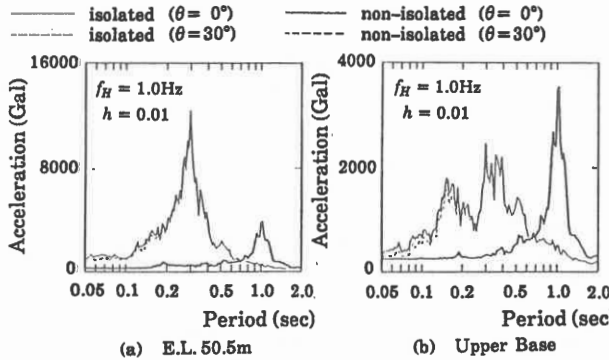
(a) Horizontal (b) Horizontal resp. generated by

tortion(at the edge of the base)

Figure 8. Maximum response accelerations due to SH waves

(a) Horizontal (b) Vertical

Figure 9. Maximum response accelerations due to SV waves

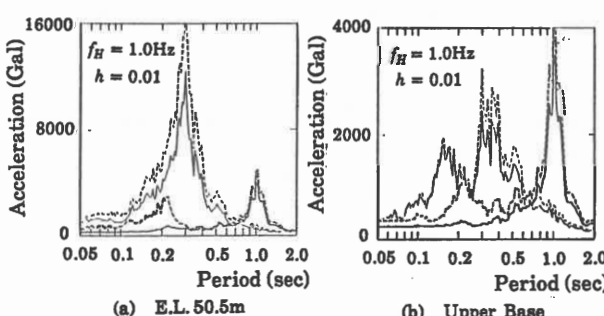


(a) E.L. 50.5m (b) Upper Base

Figure 10. Horizontal floor response spectra due to SH waves

Table 3. Maximum horizontal response due to SH waves

Case	Incident Angle $\theta^\circ$	Maximum Horizontal Response (gal)		
		at the Center of Structure	by Horizontal Motion of Upper Base	by Torsional Motion of Upper Base
Isolated ( $f_H = 1.0\text{Hz}$ )	0	260.9	240.3	3.3
	10	260.7	240.2	3.3
	20	260.4	239.9	3.2
	30	260.0	239.4	3.0
Isolated ( $f_H = 0.5\text{Hz}$ )	0	89.5	86.9	0.8
	10	89.5	86.9	0.8
	20	89.3	86.8	0.8
	30	89.1	86.7	0.7
Non-Isolated	0	818.6	281.8	155.8
	30	758.5	261.7	146.7



(a) E.L. 50.5m (b) Upper Base

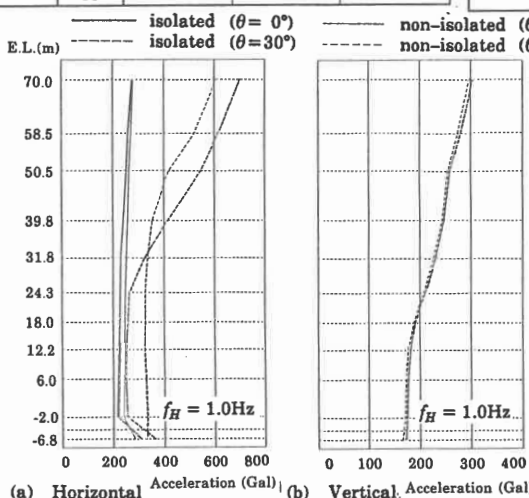
Figure 11. Horizontal floor response spectra due to SV waves

Table 4. Maximum horizontal response due to SV waves

Case	Incident Angle $\theta^\circ$	Maximum Horizontal Response (gal)		
		at the Center of Structure	by Horizontal Motion of Upper Base	by Rocking Motion of Upper Base
Isolated ( $f_H = 1.0\text{Hz}$ )	0	263.8	237.7	1.8
	10	265.8	236.7	22.0
	20	286.6	248.5	45.8
	30	417.8	331.0	150.8
Isolated ( $f_H = 0.5\text{Hz}$ )	0	89.0	86.9	0.4
	10	94.7	87.7	14.1
	20	110.6	95.3	37.6
	30	334.8	150.2	158.4
Non-Isolated	0	818.6	281.8	16.6
	30	1172.2	334.2	203.1

**Table 5. Maximum Relative displacement of isolation devices due to SH waves**

Isolation Frequency $f_H$ (Hz)	Incident Angle $\theta$ (°)	Maximum Relative Displacement		
		Horizontal Displacement at the Center (cm)	Torsional Angle ( $\times 10^{-5}$ rad)	Horizontal; Displacement at the Edge (cm)
1.0	0	6.27	0.0	6.27
	10	6.27	3.60	6.36
	20	6.26	7.09	6.44
	30	6.25	10.33	6.51
0.5	0	8.78	0.0	8.78
	10	8.78	3.25	8.82
	20	8.78	6.38	8.85
	30	8.77	9.31	8.88



**Figure 13. Maximum response accelerations**

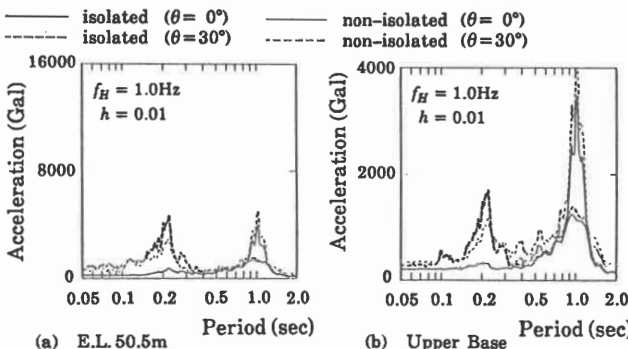


**Figure 14. Horizontal floor response spectra**

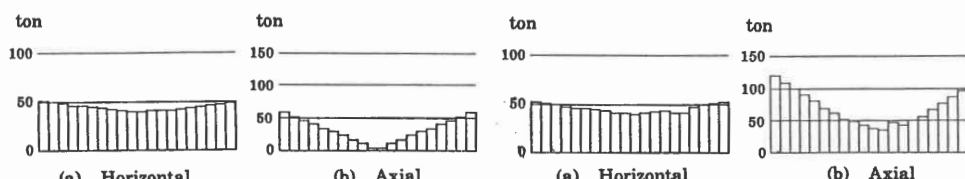


**Figure 15. Forces of isolation devices ( $\theta=0^\circ$ )**

**Table 6. Relative displacement of isolation devices due to SV waves**

Isolation Frequency $f_H$ (Hz)	Incident Angle $\theta$ (°)	Maximum Relative Displacement		
		Vertical Displacement at the Center ( $\times 10^{-2}$ cm)	Rocking Angle ( $\times 10^{-6}$ rad)	Vertical Displacement at the Edge ( $\times 10^{-2}$ cm)
1.0	0	0.0	6.21	2.48
	10	0.26	6.23	2.52
	20	0.38	6.68	2.73
	30	1.20	8.45	4.01
0.5	0	0.0	2.13	0.85
	10	0.26	2.19	0.93
	20	0.38	2.44	1.09
	30	1.20	4.86	2.49

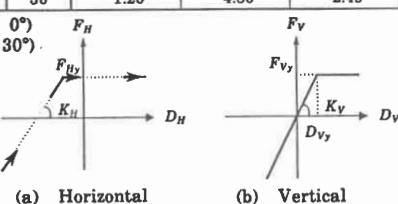


**Figure 12. Force-displacement relationships of isolation devices**

**Table 7 Maximum horizontal accelerations (E.L. 50.5m)**

Incident Angle $\theta$ (°)	Maximum Horizontal Response(gal)		
	at the Center of Structure	by Horizontal Motion of Upper Base	by Rocking Motion of Upper Base
0	252.1	215.5	16.0
10	249.4	214.8	24.0
20	257.5	228.4	41.6
30	544.2	253.7	220.6

**Table 8 Maximum Relative displacement of isolation devices**

Incident Angle $\theta$ (°)	Maximum Relative Displacement		
	Vertical Disp. at the Center ( $\times 10^{-2}$ cm)	Rocking Angle ( $\times 10^{-6}$ rad)	Vertical Disp. at the Edge ( $\times 10^{-2}$ cm)
0	0.11	5.70	2.17
10	0.34	5.70	2.24
20	0.49	5.87	2.33
30	1.55	9.33	4.29

**Figure 16. Forces of isolation devices ( $\theta=30^\circ$ )**